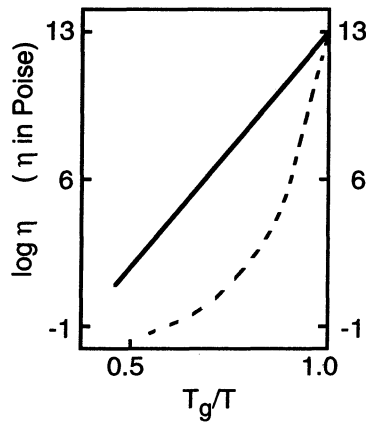


**Figure 2.4.** Schematic illustration of the volume versus temperature curve.  $T_g$ : glass transition temperature,  $T_m$ : melting temperature.

In the topological disorder seen in amorphous semiconductors, however, the short-range order is reserved in a similar way to their crystalline counterparts. As will be mentioned in Sec. 5.1, the chemical bonding theory constitutes a convenient approach to understand fundamental properties of amorphous semiconductors.

## 2.2 Glass transition

When the temperature decreases from their liquid phase, some materials do not crystallize below their melting temperature, but they become a supercooled liquid. As the temperature keeps decreasing, the so-called *glass transition* occurs at a certain temperature,  $T_g$ , below which they become glasses. These behaviours are explained by the volume versus temperature curve, as shown in Fig. 2.4. Glasses are typical examples of metastable and non-equilibrium states which are also classified as amorphous materials, as was mentioned in Chapter 1. Not all of amorphous materials, however, become glasses. Glasses exhibit the following feature as an example. Above  $T_g$ , viscosity  $\eta$  generally behaves like the following



**Figure 2.5.** Schematic illustration of the viscosity versus  $T_g/T$  curves; solid line: Arrhenius law, dashed line: non-activated-type (Yonezawa, 1991).

temperature variation which is well known as the Vogel–Fulcher law that is an experimental expression:

$$\eta = \eta_0 \exp[\text{const.}/(T - T_0)]. \quad (2.1)$$

If  $T_0 = 0$ , this expression becomes the Arrhenius law. For the case of  $T_0 \neq 0$ , as seen in Fig. 2.5, the activation energy cannot be defined definitely, namely, its value varies with temperature. This suggests that the activation process cannot be defined uniquely, but that many processes are involved. According to Angell (1988), glasses following the Arrhenius law are called *strong glasses*, while those following the Vogel–Fulcher law are called *fragile glasses*. Some examples are illustrated in Fig. 2.6. Typical examples for the former category are some oxides such as  $\text{SiO}_2$  and  $\text{GeO}_2$  with strongly-bonded network structures, while those for the latter category are ionic glasses such as  $\text{ZnCl}_2$  and  $\text{CKN}([\text{Ca}(\text{NO}_3)_2]_{0.4}[\text{K}(\text{NO}_3)]_{0.6})$ .

As is well known,  $T_g$  depends on the speed of liquefaction. This means that  $T_g$  is not uniquely determined, so that the glass tran-

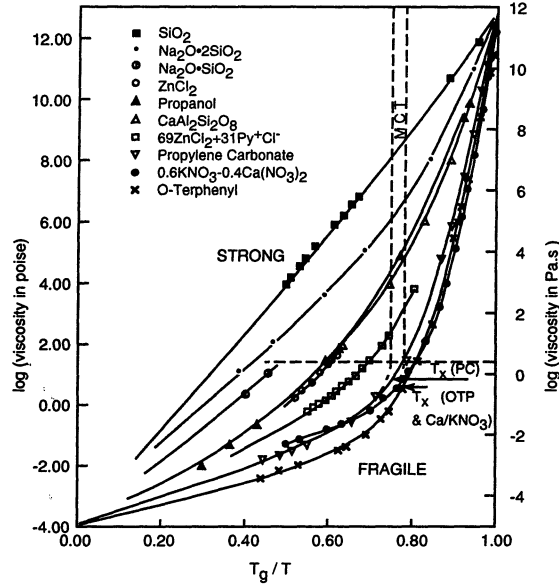


**Figure 2.6.** Viscosities of strong glasses and fragile glasses as a function of reduced reciprocal temperature  $T_g/T$ , where  $T_g$  is defined as the temperature where the viscosity is  $10^{13}$  poise (Angell, 1988).

sition is not a phase transition in the usual sense. Recently, the glass transition has been analyzed from the viewpoint of anomalous relaxation of disordered structures (Yonezawa, 1991). This type of relaxation processes has been expressed by relaxation function  $F(t)$  that is written as the stretched exponential function

$$F(t) = F_0 \exp[-(t/\tau)^\beta], \quad (2.2)$$

where  $\beta$  is the dispersive parameter ( $0 < \beta < 1$ ).

From the experimental investigations on relaxation times by inelastic scattering of neutrons (Mezei, Knaak and Farago, 1987; Knaak, Mezei and Farago, 1988) and Brillouin and Raman scatterings (Torell, Borjesson and Elmroth, 1990; Li, Du, Chen, Cummi-

nus and Tao, 1992), the existence of another transition temperature,  $T_c$ , has been suggested, as being above  $T_g$ . This temperature is associated with anomalous decrease in the Debye–Waller factor of scattering. This means that above the temperature, at which thermodynamical properties of the system change, its dynamical properties have already changed. The nature of  $T_c$  has been extensively investigated from both theoretical and experimental bases.

Computer simulations of glass transitions provide a powerful means for elucidating the nature of glass transition and changes in structural properties associated with the transition. In the following, isothermal-isobaric molecular dynamics simulations by Yonezawa, Nose and Sakamoto (1988) are described. Lennard–Jones liquid of 864 atoms (Ar) is quenched, e.g., with quench rates of  $2 \times 10^{13}$  K/s and  $4 \times 10^{11}$  K/s. The Lennard–Jones potential is given by

$$V(r) = 4\epsilon \left[ \left( \frac{\delta}{r} \right)^{12} - \left( \frac{\delta}{r} \right)^6 \right], \quad (2.3)$$

where we take values of the parameters,  $\sigma$  and  $\epsilon$ , for argon atoms as  $\sigma = 3.446 \text{ \AA}$  and  $\epsilon = 125 \text{ K}$ .

When a crystal (fcc) is heated up, the volume  $V$  increases continuously until  $T = 105 \text{ K}$ , as shown in Fig. 2.7 (solid circles). The melting point given in this computer simulation is  $105 \text{ K}$ , which is higher than that of actual Ar gas,  $84 \text{ K}$ . This is due to the fact that the number of atoms in the system is too low compared to a real system. When a liquid is cooled down, the volume decreases continuously until  $60 \text{ K}$ . For the cooling rate of  $4 \times 10^{10} \text{ K/s}$ ,  $V$  changes further as shown by small dots. This shows crystallization at about  $54 \text{ K}$ . Faster cooling rates like  $4 \times 10^{11} \text{ K/s}$  and  $2 \times 10^{13} \text{ K/s}$  exhibit glass transitions, as shown in Fig. 2.8 (enthalpy versus temperature curves), which exhibit  $T_g = 47 \text{ K}$  and  $50 \text{ K}$ , respectively. The glass state shown in the figure (solid squares) is realized by a cooling rate of  $4 \times 10^{13} \text{ K/s}$  for which  $T_g = 50 \text{ K}$  is obtained. Here,  $T_g$  is defined by the temperature at which the extrapolations of the liquid and glassy lines are intersected. This shows that when the cooling rate is faster,  $T_g$  becomes higher, as has already been mentioned.

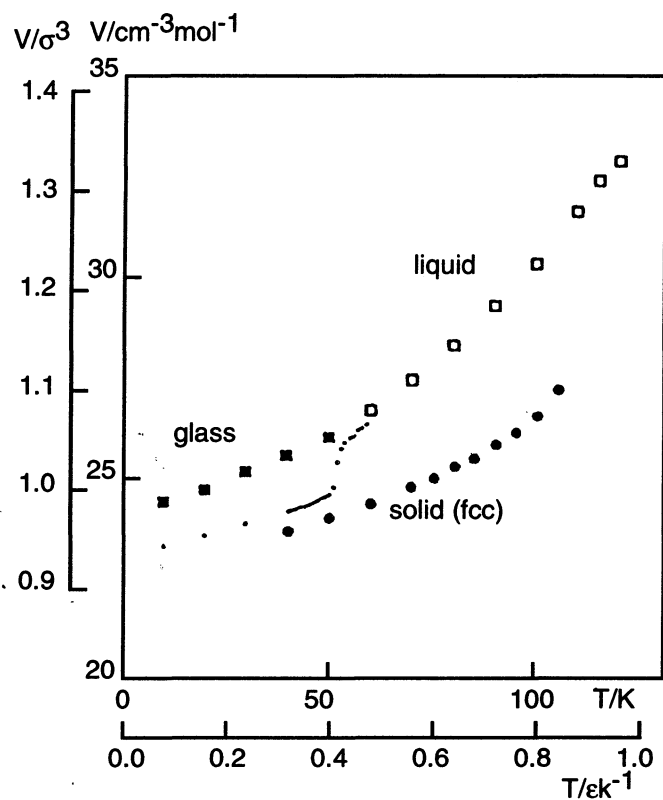


**Figure 2.7.** Volume versus temperature for crystals on heating (filled circles) and liquids (open squares). Small dots represent the cooling-crystallization process, while filled squares the glassy state (Yonezawa *et al.*, 1988).

Changes in structural properties, e.g., pair-correlation function, structural parameters etc., associated with the glass transition have also been investigated in the Lennard-Jones liquid mentioned above (Yonezawa *et al.*, 1988).

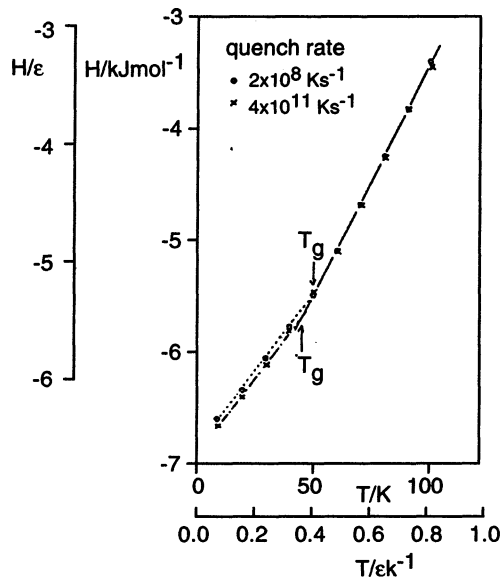


**Figure 2.8.** Entropy versus temperature curve for two cooling processes with the quenching rates of  $2 \times 10^{13}$  K/s and  $4 \times 10^{11}$  K/s (Yonezawa *et al.*, 1988).

### 2.3 Glass formation

Glass formation has been discussed for a long time from the viewpoints of thermodynamics, kinetics and structural properties (Kadoun, Chaussemy, Fornazero and Mackowski, 1983). In the case of glass formation by rapid quenching from the molten state of materials, the glass-forming ability is related to the viscosity of the melt. On cooling, viscous liquid does not provide the atomic mobility necessary for forming crystallites. Thus, when the viscosity is smaller, then glass formation becomes difficult. Indeed, the maximum glass-transition temperature in  $\text{As}_x\text{Se}_{1-x}$  is obtained for  $x = 0.4$  and this composition almost corresponds to the maximum viscosity in the whole range of  $x$ . The glass-formation region as a function of  $x$  lies in  $x < 0.57$  for  $\text{As}_x\text{Se}_{1-x}$  (see Fig. 2.9) and  $x < 0.3$  for  $\text{As}_x\text{S}_{1-x}$ . These are also related to structural properties of  $\text{As}_x\text{Se}_{1-x}$  and  $\text{As}_x\text{S}_{1-x}$ . The threefold coordinated As atoms